Whole-genome sequencing analysis of Y chromosome microdeletion: a case report

Zhixiang Gao*, Feng Yuan*, Qiaoqiao Li, Renlan Xia, Kai Fu, Boxin Xue and Xiaolong Liu

Abstract

The mechanisms by which Y chromosome microdeletions cause infertility have been well described; however, the therapeutic targets remain a challenge. Here, we used whole-genome sequencing to explore the mechanism of Y chromosome deletion and potential therapeutic targets in a patient with infertility. There were no abnormalities in the patient's medical history. Routine semen analysis showed immotile sperm and only two motile spermatozoa were occasionally see after centrifugation, indicating that the direct cause of infertility was an abnormal sperm count and motility. A Y chromosome microdeletion test revealed partial deletion of the *AZFc* region, including *AZFc1*, *AZFc2*, *AZFc3*, and *AZFc4*. Whole-genome sequencing showed that the patient had seven harmful mutations, with only one significant epigenetic mutation, *SH3KBP1*. Gene Ontology analysis of these meaningful mutations indicated involvement of cAMP signaling pathways. The patient's wife became pregnant following *in vitro* fertilization, and no significant abnormalities were found during prenatal examination. This case suggests that Y chromosome microdeletion and gene mutation may affect the cAMP signaling pathway, leading to reduced sperm quality and male infertility.

Keywords

Case report, male infertility, Y chromosome microdeletion, azoospermia, genome sequencing, genetic mutation

*These authors contributed equally to this work.

Corresponding author:
Xiao-long Liu, Department of Urology, The Second Affiliated Hospital of Soochow University, 1055 Sanxiang Road, Suzhou, Jiangsu 215000, China.
Email: liurol@163.com

Department of Urology, The Second Affiliated Hospital of Soochow University, Suzhou, China

Introduction

The human reproductive system affects the health of the offspring, and is susceptible to environmental exposure. Recent increases in workplace stress and environmental pollution have severely affected human reproductive health, with male infertility becoming a global health problem.[1,2] The main causes of male infertility are reduced sperm quality and impaired sperm function.[1] Evolutionarily, spermatozoa are the most divergent cell type, possibly as a consequence of their need to perform their function outside the male body, in the female reproductive tract.[3] Spermatogenesis occurs in the testes, and spermatozoa are morphologically intact but functionally immature when they leave the testes. To achieve their goal, spermatozoa thus need to undergo maturation and capacitation in the epididymis, followed by the acrosome reaction in the female reproductive tract. These are interdependent processes, and any errors could lead to abnormal morphology or sperm dysfunction.[4] Although spermatogenesis and sperm maturation are strictly regulated through complex signal transduction pathways, an in-depth understanding of these is currently lacking.[5] Spermatogenesis is controlled by azoospermia factor (*AZF*) genes on the long arm of the Y chromosome, and deletion or mutation of these genes may cause spermatogenesis disorders and consequent male sterility. Previous studies suggested that *AZF* deletions were the second most common genetic cause of azoospermia and oligospermia, accounting for about 3% to 29% of patients.[6] We report the case of a patient with Y chromosome microdeletion. Based on his clinical symptoms and genetic alterations, we aimed to analyze the mechanisms underlying sperm dysfunction and provide clues for the diagnosis and treatment of similar cases.

Case report

A 28-year-old male patient was admitted to our hospital with a 3-year history of reproductive failure. He had normal development, and the couple had regular sexual intercourse with endovaginal ejaculation and no contraception. The patient had no history of mumps or other specific viral infections, trauma or surgery, chronic diseases (such as hypertension and diabetes), and no family history of genetic diseases. His partner had no obvious abnormalities. Further examination showed normal development of the external genitalia, small bilateral testes, no obvious masses, and no obvious abnormality of the bilateral epididymides or spermatic cords.

B-scan ultrasonography of the prostate, seminal vesicles, testes, epididymides, and spermatic cords was carried out using a Siemens Acuson X150 ultrasound device (Siemens Healthcare, Erlangen, Germany). The patient was placed in a supine position with the lower abdomen fully exposed and the probe surface was modified with a coupling agent and placed on the symphysis. Color Doppler ultrasound examination indicated slightly smaller testes on both sides, no obvious abnormalities in the bilateral epididymides, slightly enlarged inner diameter of the left spermatic cord, no abnormalities of the seminal vesicles, a slightly enlarged prostate, and normal blood flow signals in the prostate (Figures 1 and 2).

We also evaluated sex hormone levels, semen quality, presence of anti-sperm antibody, viral infections, blood karyotype, and Y chromosome microdeletion.

Semen was harvested after 3 days of ejaculatory abstinence and liquefied at room temperature for 30 minutes. The color (yellowish-white), viscosity (moderate), pH (pH = 7), and volume (5 mL) were normal. Routine semen-quality analysis (Huijia, Beijing, China) detected no sperm.
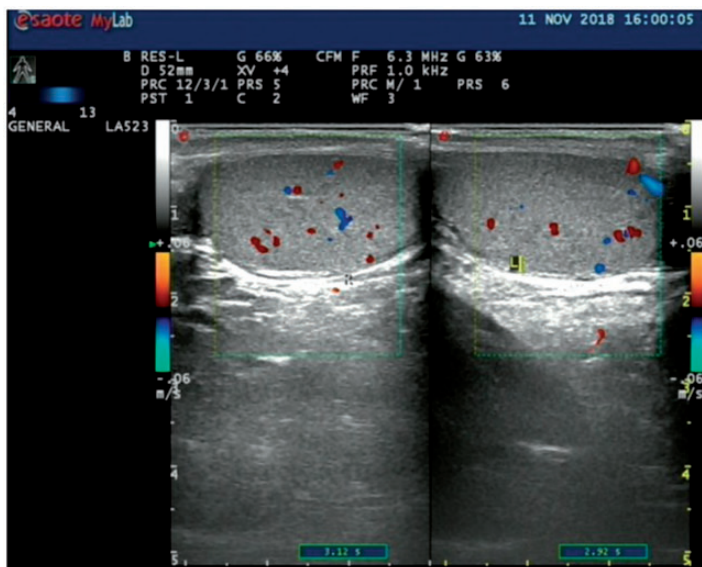
Figure 1. B-scan ultrasonography of the testes.

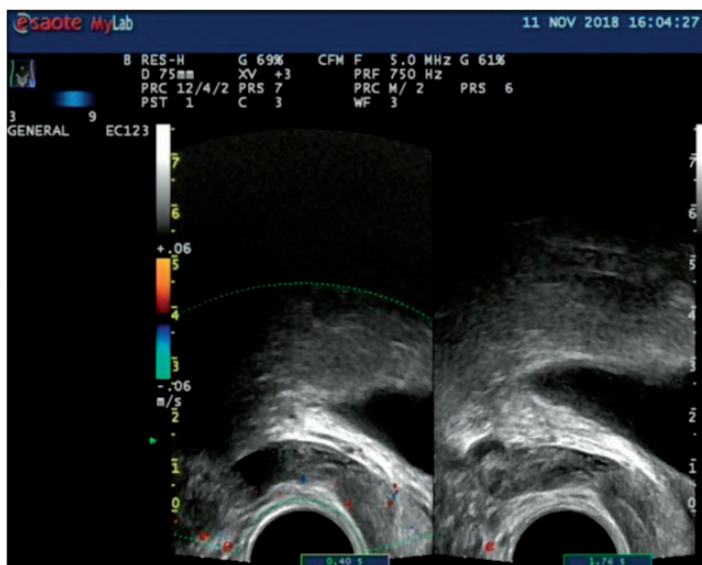**Figure 2.** B-scan ultrasonography of the seminal vesicles.

Immotile sperm and two motile spermatozoa were occasionally seen after centrifugation.

Based on the abnormal semen analysis, we examined the patient's hormones levels to further investigate the cause of his azoospermia. Peripheral blood was harvested at 8:00 am and testosterone, estradiol, progesterone, prolactin, luteinizing hormone,

follicle-stimulating hormone, sex hormone binding globulin, and dehydroepiandroster-one sulfate levels were assessed using a Cobas e601 analyzer (Roche, Switzerland). The results were within normal ranges (Table 1).

We also collected peripheral blood and tested for the presence of anti-sperm IgG, IgA, and IgM antibodies using Kanghua ELISA kits (Kanghua, Shandong, China) and for viral immunological response by detecting IgM and IgG antibodies against rubella virus, cytomegalovirus, *Toxoplasma*, and herpes simplex virus type 2 using Aikang ELISA kits (ACON, Hangzhou, China). The results were all normal (Table 2).

We collected peripheral blood and extracted DNA for karyotype analysis and to evaluate Y chromosome microdeletion. Karyotype analysis showed 46, XY, and no obvious abnormalities were observed by G-banding (Figure 3). Detection of Y chromosome microdeletion confirmed that the male sex-determining gene *SRY* was not affected. DNA samples were submitted for analysis on a MassARRAY nucleic acid mass spectrometer (Agena Bioscience, CA, USA) to detect sequence tagged sites (STS) in the *AZFa* (sY84/sY86), *AZFb* (sY121/sY127/sY134), and *AZFc* (sY160/sY252/sY255/sY1191/sY1291) regions of the Y chromosome. Partial deletions (AZFc1-4) in the *AZFc* region were detected, with no deletion of *AZFc5* (Table 3 and Figure 4).

Library construction and genome sequencing were performed by Beijing Novogene Co., Ltd. The integrity and purity of the DNA samples were determined by agarose gel electrophoresis. DNA concentration was determined with a Qubit 3.0 fluorometer (Thermo Fisher Scientific, MA, USA), and samples containing more than $0.5\,\mu g$ DNA were used for library construction. A DNA library was constructed by disruption of the genomic DNA into ~350-bp fragments using a Covaris crusher (Covaris, MA, USA), end-repair, and poly(A) tailing, followed by adapter ligation at both ends.

Table 2. Immunological analysis.

Antibody	Positive/negative
Anti-sperm IgG	−
Anti-sperm IgA	−
Anti-sperm IgM	−
Anti-rubella virus IgM	−
Anti-cytomegalovirus IgM	−
Anti-toxoplasma IgM	−
Anti-herpes simplex virus type 2 IgM	−
Anti-rubella virus IgG	+
Anti-cytomegalovirus IgG	+
Anti-*Toxoplasma* IgG	−
Anti-herpes simplex virus type 2 IgG	−

Table 1. Sex hormone determination.

Hormone	Patient level	Normal range	Units
Estradiol	13.94	7.63–42.60	pg/mL
Progesterone	0.22	0.00–0.157	ng/mL
Prolactin	23.57	4.04–15.20	ng/mL
Testosterone	403.80	249.00–836.00	ng/mL
Luteinizing hormone	6.62	1.70–8.60	mIU/mL
Follicle-stimulating hormone	16.17	1.50–12.40	mIU/mL
Sex hormone binding globulin	3.39	1.38–4.60	μg/mL
Dehydroepiandrosterone sulfate	237.90	85.00–690.00	μg/dL

Figure 3. Karyotype analysis of the peripheral blood.

Table 3. Y chromosome microdeletion detection.

Region	No.	STS site	Detection
AZFa	1	sY84	Exist
	2	sY86	Exist
AZFb	1	sY121	Exist
	2	sY127	Exist
	3	Sy134	Exist
AZFc	1	sY160	Deletion
	2	sY254	Deletion
	3	sY255	Deletion
	4	sY1191	Deletion
	5	sY1291	Exist

STS, sequence tagged site.

The quality of the library was evaluated using a Qubit 2.0 fluorometer, and the insert size was detected with NGS3K/Caliper (Novogene Co., Ltd., Beijing, China). Finally, quantitative polymerase chain reaction was performed to quantify the effective concentration of the library (3 nM).

After library quality assessment, DNA sequencing was performed using the Illumina platform (Integrated DNA Technologies, Inc., Coralville, IA, USA) according to the effective concentration and data output requirements. Sequencing data quality was assessed in terms of sequencing error rate, data volume, and comparison rate. If sequencing data met the standards, subsequent analysis was performed; otherwise, the library was rebuilt and tested. Evaluation of the base distribution showed no separation of AT and GC, and the sequencing data met the experimental requirements. The sequencing depth was $30\times$, and the chromosome coverage was 100%, except for the Y chromosome (Figure 5).

Raw sequenced reads were then processed and variations were detected by aligning high-quality sequences to the human reference genome GRCh37/hg19, followed by statistics and annotation. However, such tests generate massive data and relevant disease-related mutations are limited. The mutation detection results were thus used to screen for pathogenic mutation sites/genes and predict disease correlations.[7,8]

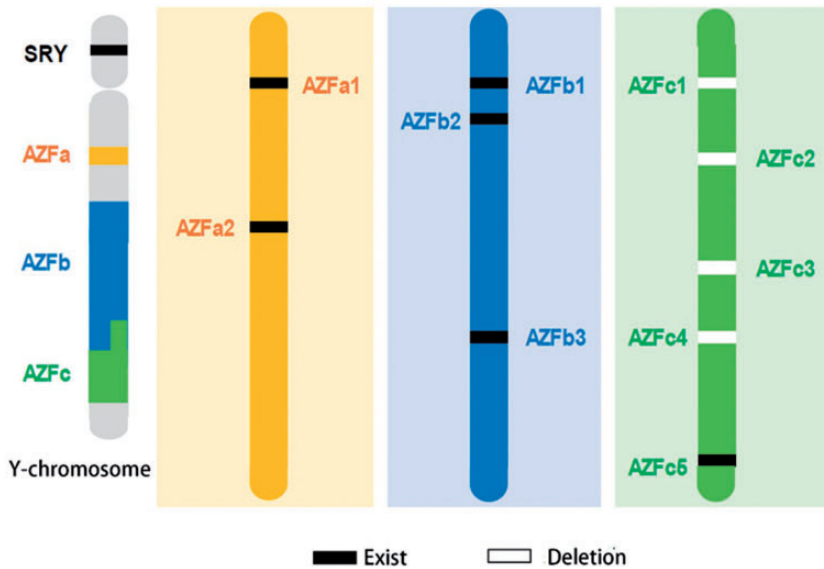First, potentially pathogenic or splicing-affecting single nucleotide polymorphism/InDel mutations were screened and

Figure 4. Male Y chromosome microdeletion report and explanatory chart.
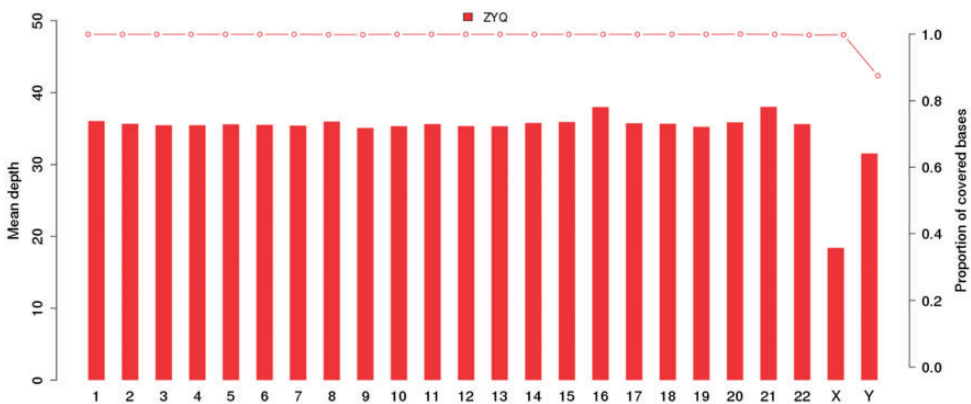

Figure 5. Coverage depth (left coordinate) and coverage (right coordinate) for each chromosome.

classified according to the American College of Medical Genetics and Genomics 2015 classification criteria (Table 4). Five pathogenic mutations (*KDM2A*, *ACOX1*, *NEB*, *PREX1*, and *RNF168*) were identified (Table 5). Given that the noncoding region plays critical roles in gene regulation, variations in the noncoding regions were screened (Table 6).

Genomiser software screening identified 574,029 non-coding region variants related to disease or phenotype. The conserved sites were identified by Combined Annotation Dependent Depletion and Genome Wide Annotation of VAriants, and 3714 candidate sites were obtained. Finally, we used the GTEx, Roadmap, and Encode databases to screen for variants that

Table 4. Screening of single nucleotide polymorphism/InDel pathogenic mutations.

Total	Pathogenic	Likely pathogenic	VUS	Likely benign	Benign
25,596	5	3	1231	1231	23124

VUS, variations of unknown significance.

Table 5. Annotation of pathogenic mutations.

ACMG	Priority	Chromosome	Position	ID	Ref	ALT	Qual	Gene
PVS1, PM2, PP3	H	11	66888833	rs757032822	A	C	222	*KDM2A*
PVS1, PM1, PM2, PP3	H	17	73947496		C	A	209	*ACOX1*
PVS1, PM2, PP5	H	2	152397984	rs749452641	G	A	222	*NEB*
PVS1, PM2, PP3	H	20	47254290		T	C	198	*PREX1*
PVS1, PM2, PP3	H	3	196202101	rs750269822	C	T	207	*RNF168*

ACMG, evidence level of American College of Medical Genetics and Genomics; Position, absolute position of variation sites in the chromosome; ID, dbSNP annotation ID; Ref, reference; ALT, sample genome base; Qual, variation score, positively correlated with quality; H, high.

Table 6. Variations in the noncoding region.

Genomiser	GnomAD_EAS_AF	Conservation	Epigenome
574,029	8291	3714	1

Genomiser, variation counts in the noncoding region using Genomiser; Conservation, conserved variation counts by Combined Annotation Dependent Depletion and Genome Wide Annotation of VAriants screening; Epigenome, variation sites affecting gene expression with DNA functional elements screened by GTEx, Roadmap, and Encode databases.

might affect gene expression in specific tissues, and annotated them as DNA functional elements. After screening, the important noncoding gene, *SH3KBP1*, was identified and annotated (Table 7).

In living organisms, genes exert their biological functions cooperatively, and phenotypic differences in complex diseases may be caused by mutations in multiple genes. The major metabolic and signaling pathways affected by genetic mutations can be determined through functional enrichment analysis. We therefore carried out Gene Ontology (GO) enrichment analysis to identify the mutations involved in cell component, biological pathway, and molecular function. The results are shown in Figure 6. We also carried out Kyoto Encyclopedia of Genes and Genomes analysis. A scatter plot of KEGG pathways indicated that the variant genes were mainly involved in the cAMP signaling pathway (Figure 7). *P* values were calculated using hypergeometric distribution and bioinformatics software (R; http://www.R-project.org/).

The final diagnosis in the present case was male infertility due to Y chromosome microdeletion and genetic mutations. Considering that the patient had few active sperm, we recommended *in vitro* fertilization. The couple underwent pre-implantation genetic diagnosis to select normal embryos for implantation with the aim of improving the clinical pregnancy rate. The patient's wife subsequently
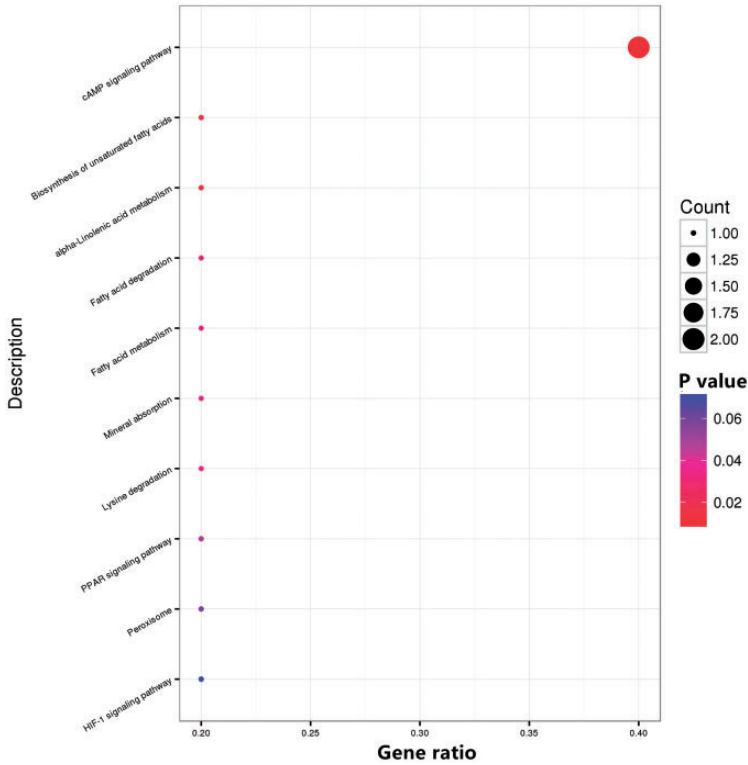
Table 7. Identification and annotation of variations in the noncoding region.

Chr	Position	ID	Ref	ALT	Qual	Filter	Gene	Description	Function
X	19903991	rs5955861	A	G	225	PASS	SH3KBP1	SH3-domain kinase-binding protein 1	intronic

HR, chromosome; ID, dbSNP annotation ID; Ref, reference; ALT, sample genome base; Qual, variation score, positively correlated with quality.

Figure 6. Gene Ontology (GO) functional enrichment scatter plots. (a) Cell component, (b) biological pathway, and (c) molecular function. X-axis indicates the ratio of genes mapped to that pathway to total genes; y-axis indicates enriched GO terms; dot size indicates number of genes mapped to the GO term; and color indicates *P*-value.

Figure 7. Scatter plot of Kyoto Encyclopedia of Genes and Genomes (KEGG) pathway analysis. X-axis represents ratio of genes mapped to that pathway to total genes; y-axis represents name of enriched KEGG pathway; dot size indicates number of genes mapped to the pathway; and color indicates P-value.

became pregnant and the fetus was growing well, with no obvious abnormalities during prenatal examination.

The patient provided consent for the treatment and for the publication of the case report and accompanying images. We have de-identified all patient details.

Discussion

Infertility can be caused by abnormalities in sperm development, morphology, and motility, which in turn depend on metabolic and signaling pathways. Defects in genes involved in these metabolic and signal transduction pathways may thus lead to sperm dysfunction and infertility.

The current patient was admitted with infertility; however, no congenital abnormalities of the reproductive system and no significant alterations in laboratory tests, such as androgen levels, were identified. Nevertheless, no spermatozoa were detected by routine semen analysis, and only two motile sperm were seen occasionally after centrifugation, indicating that the direct cause of infertility was abnormal sperm count and motility. Chromosome karyotyping detected the Y chromosome, and the *AZFc* region contained microdeletions of *AZFc1*, *AZFc2*, *AZFc3*, and *AZFc4*. Y chromosome microdeletions are the second most frequent genetic cause of male infertility. However, there are also individual differences in terms of the effects

of these microdeletions, and the exact mechanism of their action in relation to male infertility remains unknown. The role of AZFc microdeletion in infertility is particularly unclear.

Genomic sequencing in the current patient identified seven harmful mutations, including *KDM2A*, *ACOX1*, *NEB*, *PREX1*, and *RNF168*, as well as a sense epigenetic mutation in *SH3KBP1*. GO analysis of these sense mutations mapped to the cAMP signal pathway, which is widely recognized as a regulator of mammalian sperm cell motility. Activation of the CatSper channel is required for calcium entry into sperm. HCO_3^{-} and Ca^{2+} regulate atypical sperm adenylyl cyclase, leading to production of cAMP and activation of protein kinase A (PKA), which in turn induces phosphorylation of axonemal dynein, leading to depletion of ATP and increased intracellular pH. PKA activates serine threonine tyrosine kinase, triggering a phosphorylation cascade of proteins related to sperm motility.[9] Moreover, sperm capacitation is mainly regulated through the cAMP-dependent PKA-mediated protein phosphorylation cascade.[10] Binding of PKA regulatory subunits to the A-kinase anchoring protein family promotes tyrosine phosphorylation of sperm proteins by indirectly activating tyrosine kinases. Protein tyrosine phosphorylation of AKAP proteins (AKAP3 and FSP95) in human spermatozoa is critical for sperm capacitation. Tyrosine kinase receptors are transmembrane proteins with an extracellular ligand-binding domain and an intracellular tyrosine kinase domain. Upon extracellular ligand binding, these receptors activate and undergo autophosphorylation or phosphorylate other proteins. Tyrosine phosphorylation of sperm flagellin results in human sperm capacitation. Elucidation of the specific pathogenic mechanism could enable the development of targeted therapies, such as specific agents to improve

sperm motility.[11,12] As such, altering cAMP metabolism using phosphodiesterase inhibitors was reported to increase sperm motility in human spermatozoa.[13] *In vitro* fertilization represents a good option for men with severe sperm loss,[14] while additional preimplantation genetic diagnosis can avoid inherited problems in the next generation.

A reduced sperm count and function could thus be attributed to Y chromosome microdeletions and genetic mutations, eventually leading to infertility. However, this was based on a single case and individual differences cannot be ruled out, and the results thus need to be validated by further screening in large samples. Furthermore, the relationship between the Y chromosome microdeletion and the genetic mutations is unknown, and further studies are needed to identify the specific mechanism.

Conclusion

We applied whole-genome sequencing to investigate Y chromosome deletions and explore related gene mutations in a patient with male infertility. Several gene mutations were detected, and GO analysis found that these mutations were mainly mapped to the cAMP signal pathway, indicating that abnormalities in this signaling pathway may affect sperm production and capacitation, resulting in male infertility. However, further research is needed to clarify the mechanisms involved, including the relationship between Y chromosome microdeletions and related gene mutations, to help clinicians provide targeted treatment.

ORCID iD

Xiaolong Liu 🔴 https://orcid.org/0000-0001-7136-4299

References

1. Urdinguio RG, Bayón GF, Dmitrijeva M, et al. Aberrant DNA methylation patterns of spermatozoa in men with unexplained infertility. *Hum Reprod* 2015; 30: 1014–1028.

2. Boissonnas CC, Jouannet P and Jammes H. Epigenetic disorders and male subfertility. *Fertil Steril* 2013; 99: 624–631.

3. Inaba K. Sperm flagella: comparative and phylogenetic perspectives of protein components. *Mol Hum Reprod* 2011; 17: 524–538.

4. García-Vázquez FA, Gadea J, Matás C, et al. Importance of sperm morphology during sperm transport and fertilization in mammals. *Asian J Androl* 2016; 18: 844–850.

5. Freitas MJ, Vijayaraghavan S and Fardilha M. Signaling mechanisms in mammalian sperm motility. *Biol Reprod* 2017; 96: 2–12.

6. Skaletsky H, Kuroda-Kawaguchi T, Minx PJ, et al. The male specific region of the human Y chromosome is a mosaic of discrete sequence classes. *Nature* 2003; 423: 825–837.

7. Piñero J, Bravo À, Queralt-Rosinach N, et al. DisGeNET: a comprehensive platform integrating information on human disease-associated genes and variants. *Nucl Acids Res* 2017; 45: D833–D839.

8. Yang H, Robinson PN and Wang K. Phenolyzer: phenotype-based prioritization of candidate genes for human diseases. *Nat Methods* 2015; 12: 841–843.

9. Nolan MA, Babcock DF, Wennemuth G, et al. Sperm-specific protein kinase A catalytic subunit $C\alpha^2$ orchestrates cAMP signaling for male fertility. *Proc Natl Acad Sci USA* 2004; 101: 13483–13488.

10. Bajpai M and Doncel GF. Involvement of tyrosine kinase and cAMP−dependent kinase cross−talk in the regulation of human sperm motility. *Reproduction* 2003; 126: 183–195.

11. Kumar R, Gautam G and Gupta NP. Drug therapy for idiopathic male infertility: rationale versus evidence. *J Urol* 2006; 176: 1307–1312.

12. Moein MR, Khalili MA and Davoudi A. The effect of oral administration of Pentoxifylline on sperm motility of asthenozoospermic ejaculates from men with or without testicular varicoceles. *Iran J Reprod Med* 2005; 3: 25–29.

13. Yunes R, Fernandez P, Doncel GF, et al. Cyclic nucleotide phosphodiesterase inhibition increases tyrosine phosphorylation and hyper motility in normal and pathological human spermatozoa. *Biocell* 2005; 29: 287–293.

14. Pan MM, Hockenberry MS, Kirby EW, et al. Male infertility diagnosis and treatment in the era of in vitro fertilization and intracytoplasmic sperm injection. *Med Clin North Am* 2018; 102: 337–347.